Materials Transactions, Vol. 61, No. 6 (2020) pp. 1063 to 1069

Atomic Simulations of Interactions between Edge Dislocations and a Twist Grain Boundary in Mg

Naoki Miyazawa[1,*], Shunya Suzuki[2], Masakata Hakamada[2] and Mamoru Mabuchi[2]

[1]*Department of Materials Science and Engineering, School of Materials and Chemical Technology, Tokyo Institute of Technology, Yokohama 226-8502, Japan*
[2]*Graduate School of Energy Science, Kyoto University, Kyoto 606-8501, Japan*

The roles of mechanical size and chemical bonding effect of segregated elements in grain boundaries (GBs) on the interactions between the GBs and dislocations are still not well understood. Because a twist GB tends to have a higher GB energy than a tilt GB owing to its random structure, the mechanical and chemical effects of solute elements on the dislocation-GB interactions in a twist GB are generally different from those in a tilt GB. In addition, dislocation emission from a GB in hcp metals is more complex than that in fcc metals because of the intense plastic anisotropy in hcp metals. In this study, interactions between basal ⟨a⟩ edge dislocations and a twist GB were studied in non-segregated and Al- and Fe-segregated twist Mg GBs by molecular dynamics simulations. The simulations showed that a prismatic dislocation was emitted from the GB after two basal dislocations were adsorbed into the GB. Dislocation adsorption into the GB was enhanced by Al and Fe segregation, but dislocation emission from the GB was suppressed by the segregation. Analyses of the GB width and potential energy suggested that the dislocation adsorption was mainly determined by mechanical effects, while dislocation emission strongly depended on chemical effects.
[doi:10.2320/matertrans.MT-M2020011]

(Received January 7, 2020; Accepted March 30, 2020; Published May 25, 2020)

Keywords: *Mg alloys, molecular dynamics simulations, grain boundaries, segregation*

1. Introduction

Many studies have been conducted on the effects of segregated elements on grain boundary (GB) plasticity. For example, GB fracture[1,2] and dislocation adsorption and emission at a GB[3] have been studied using first-principles (FP) simulations or molecular dynamics (MD) simulations. While these studies have emphasized the importance of mechanical size and chemical bonding effects, the effects of segregated elements on interactions between a dislocation and a GB are not yet well understood.

Most of the work on interactions between dislocations and GBs has focused on segregated[3,4] and non-segregated[5–8] tilt GBs, which have periodic structures containing compressive and extension sites. Atoms with larger atomic radius than host atoms tend to segregate into the extension sites, while smaller atoms segregate into the compressive sites in segregated GBs, resulting in a reduction in GB energy and the periodic segregation of solute atoms.[9] This size-based segregation enhances resistance against dislocation adsorption and emission.[3] In addition, the chemistry of segregated atoms can reduce the binding energy between segregated and host atoms, and thus suppress dislocation movement.[3] Therefore, both mechanical and chemical effects can increase the stability of a GB and enhance the resistance against dislocation adsorption into the GB and emission from the GB in tilt GBs. In high-energy GBs such as twist GBs, however, mechanical and chemical effects do not necessarily enhance resistance against dislocation adsorption and emission.

Interactions between edge dislocations and twist GBs are poorly understood, although some MD simulation studies of fcc metals have been conducted.[10,11] To the best of our knowledge, MD simulations for interactions between edge dislocations and twist GB have not been studied in hcp metals. Magnesium (Mg) and its alloys are representative hcp metals that are widely used in automobiles, airplanes, and other applications because of their high specific strengths. The critical resolved shear stress for basal slip is much lower than that for prismatic and pyramidal slips in Mg, and intense plastic anisotropy complicates the interactions between dislocations and GBs, especially in dislocation emission from a twist GB.

In this study, MD simulations were performed on non-segregated and Al- and Fe-segregated twist GBs in Mg to investigate the interactions between edge dislocations and twist GBs. The simulations showed that a prismatic dislocation was emitted from the GB after the adsorption of two basal edge dislocations. Dislocation adsorption into the GB was enhanced by Al and Fe segregation, but dislocation emission from the GB was suppressed by the segregation. Previous work[11] showed that the interactions between dislocations and GBs were determined by the GB energy in fcc metals. In this study, however, the interactions could not be adequately explained by the GB energy. Our results suggest that dislocation adsorption is mainly determined by mechanical effects, while dislocation emissions strongly depend on chemical effects.

2. Methods

Preliminary calculations using small models were performed to determine the stable twist angle of $[\bar{1}010]$ axis in Mg (see Fig. 1). In the small model, the cell contained about 40,000 atoms and Grain 2 was gradually rotated from 90° to 100° in increments of 0.5°. The model was relaxed for 1 ns using MD simulation. A periodic boundary condition is applied in the y direction. To investigate the effect of free surfaces, additional calculations were repeated on the cell containing about 60,000 atoms. As a result, the tendencies of energy difference for the cell containing 60,000 atoms were

*Corresponding author, E-mail: miyazawa.n.ac@m.titech.ac.jp

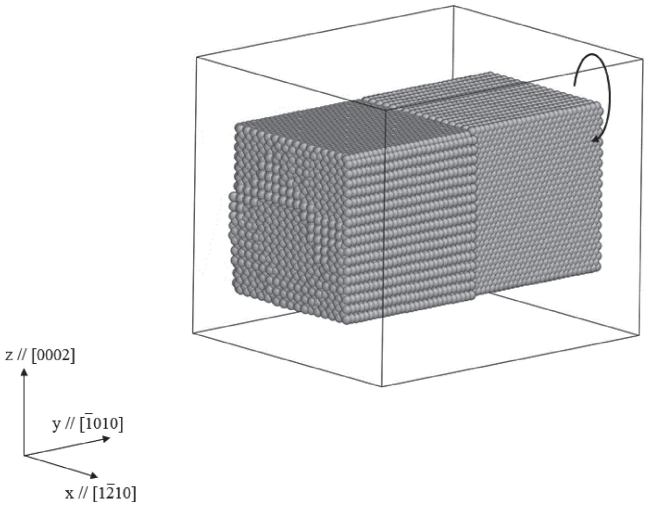

Fig. 1 Small grain-boundary model for calculation of energy difference.

almost the same as those obtained for the cell containing 40,000 atoms, for example, the rotation angle for the energetically stable GB (= 93.5°) for the cell containing 60,000 atoms was the same as that for the cell containing 40,000 atoms. Thus, we concluded that the effect of free surface was less than the effect of applied stress in the present work. A [$\bar{1}$010] twist GB model of Mg was used to investigate interactions between edge dislocations and the twist GB. Note that simulation models for calculating energy difference and dislocations-GB interactions were different. The Mg GB model used is shown in Fig. 2. The rotation angle between Grain 1 and Grain 2 was determined to be 93.5°, as explained in the Results section. The simulation cell contained about 630,000 atoms, and the size of the cell was about 8.9 × 83.9 × 19.8 nm in the x, y and z directions. The distances between GB1-2 and GB 1′-2 were about 60 and 20 nm, respectively. A periodic boundary condition is applied in the x and y direction. Additional calculations of MD shear tests were carried out on the cell containing about 1,270,000 atoms to investigate the cell size dependency. As a result, the dislocation adsorption behaviors for the cell containing 1,270,000 atoms were almost the same as those for the cell containing 630,000 atoms, for example the applied stress for adsorption of first dislocation for the former (= 100 MPa) was the same as that for the latter.

Al- and Fe-segregated GB models were constructed by substituting Mg atoms with Al or Fe atoms in the non-segregated GB model. Mg atoms in compressive sites located within ±4 Å from the GB2 plane were substituted in ascending order of Voronoi volume because the atomic radii of Al and Fe are smaller than those of Mg. The compressive sites were defined as those with a Voronoi volume below 23.2 Å^3 because the Voronoi volume of an Mg atom in a perfect single crystal is 23.2 Å^3. The concentration of Fe or Al was set to be 0.2 atom% for high-concentration models and 0.1 atom% for low-concentration models. The segregated atoms were positioned only near the GBs and not in bulk regions. The segregation sites of Al and Fe in GB2 are depicted in Fig. 3.

All MD simulations were performed at 5 K on the twist Mg GB models. The parallel MD code LAMMPS[12] was used with the modified embedded-atom method (MEAM) potential[13] in the NVT ensemble. The time step was 1 fs in all calculations. The Atomeye[14] and OVITO[15] software packages were used to visualize the simulation results. In the visualizations, the atoms are coloured according to their potential energies and by common neighbour analysis (CNA).[16] In the illustrations with CNA, light blue, blue, and brown spheres indicate atoms whose local configurations are hexagonal close packed (hcp), face-centred cubic (fcc), and neither hcp nor fcc, respectively.

Edge dislocations were generated at the centre of Grain 1 based on the procedure proposed by Osetsky *et al.*[17] After generating one edge dislocation, the cell was relaxed by MD simulation for 3 ns with the two outermost layers of the cell in fixed positions. The potential energy was minimum after 1 ns simulations. After the relaxation, two Shockley partial dislocations with Burgers vectors of 1/3⟨$\bar{1}$100⟩ and stacking faults between them were generated (Fig. 2). In the present study, the Burgers vectors and dislocation lines were determined using Dislocation Extraction Algorithm (DXA) analysis[18,19] in OVITO software.[15] Every 100 ps, an incremental stress of 50 MPa was applied in the y-direction

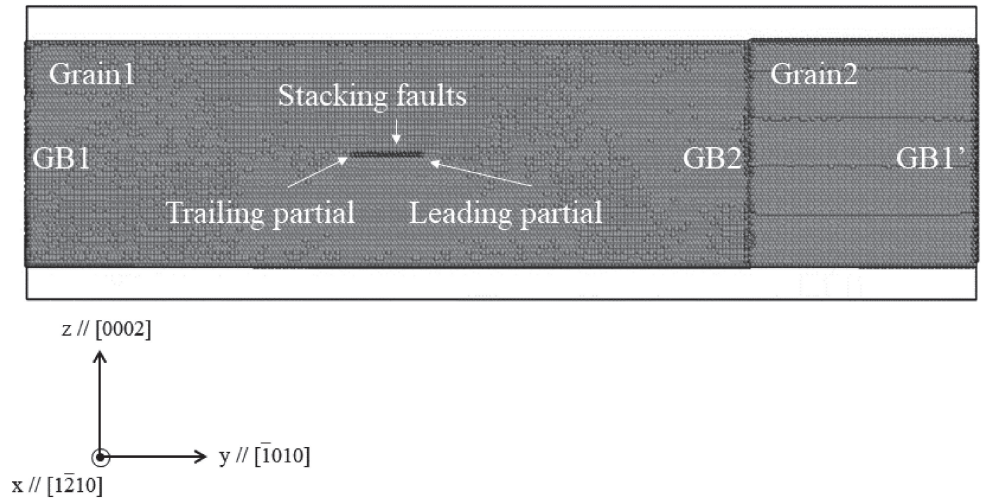

Fig. 2 A [$\bar{1}$010] twist Mg grain boundary cell. A periodic boundary condition is applied in the x and y direction.

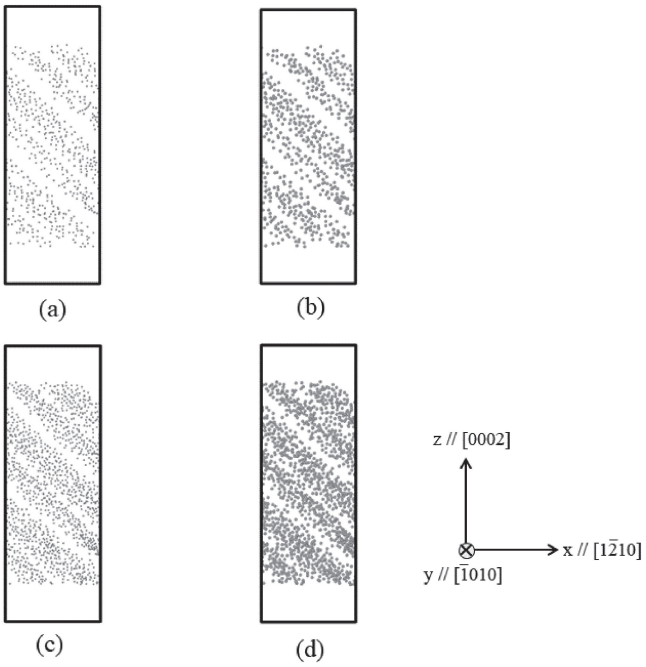

Fig. 3 Segregation sites in grain boundaries: (a) low-concentration Fe-segregated GB, (b) low-concentration Al-segregated GB, (c) high-concentration Fe-segregated GB, and (d) high-concentration Al-segregated GB, where the orange and pink spheres represent Fe and Al atoms, respectively.

on the *xy* plane of the GB model to move the partial dislocations to the GB. The stress was achieved by applying vectoral force on the top two outermost layers. The high stresses of ~900 MPa which were much higher than the yield stress of Mg were applied in the present simulations. This is because the simulation model corresponded to a nano-crystalline model with the grain size of 60 nm.

We calculated the GB energy because it may affect the dislocation-GB interactions. The GB energy of a non-segregated GB can be calculated by

$$\gamma_{\mathrm{GB}} = (E_{\mathrm{GB}} - E_{\mathrm{bulk}})/A_{\mathrm{GB}} \tag{1}$$

where γ_{GB} is the GB energy of a non-segregated GB, E_{GB} is the internal energy of a model non-segregated GB, E_{bulk} is the internal energy of a model bulk solid with the same chemical composition as the model non-segregated GB, and A_{GB} is the total area of the non-segregated GB. The GB energy of a segregated GB can be calculated by[20,21]

$$\gamma_{\mathrm{seg.GB}} = (F_{\mathrm{seg.GB}} - F_{\mathrm{seg.bulk}})/A_{\mathrm{seg.GB}} \tag{2}$$

where $\gamma_{\mathrm{seg.GB}}$ is the GB energy of a segregated GB, $F_{\mathrm{seg.GB}}$ is the formation energy of a model segregated GB, $F_{\mathrm{seg.bulk}}$ is the formation energy of a model bulk solid with the same chemical composition as the segregated GB model, and $A_{\mathrm{seg.GB}}$ is the total area of the segregated GB. The formation energy of a model solid is given by

$$F = E - (\varepsilon_{\mathrm{bulk,matrix}} N_{\mathrm{matrix}} + \varepsilon_{\mathrm{bulk,seg}} N_{\mathrm{seg}}) \tag{3}$$

where F is the formation energy of the model, E is the total energy of the model, $\varepsilon_{\mathrm{bulk,matrix}}$ is the internal energy of a matrix atom in a pure bulk model, $\varepsilon_{\mathrm{bulk,seg}}$ is the internal energy of a segregated atom in a bulk model consisting of segregated atoms, and N_{matrix} and N_{seg} are the respective numbers of matrix and segregated atoms in each model. It is difficult to completely eliminate effects of free surface on the GB energy. However, because all the models used in the present work contained the free surface with the same crystal orientation and the same surface area, the tendency of GB energy should be valid.

3. Results

The energetics of [$\bar{1}$010] twists Zn GBs were investigated by Faraoun *et al.*,[22] who found that a twist GB with an angle of 93° was the energetically stable in Zn except for CSL GB. In this study, the energy difference[22] of [$\bar{1}$010] twist Mg GB was calculated to investigate the stable rotation angle of Mg using a small twist GB model, where the energy difference, E_{dif}, is defined by

$$E_{dif} = E_{GB}/N_{GB} - E_{BULK}/N_{BULK} \tag{4}$$

where E_{GB} is the internal energy of a GB model, N_{GB} is the number of atoms in the GB model, E_{BULK} is the internal energy of a bulk model and N_{BULK} is the number atoms in the bulk model. Figure 4 shows an energy difference of the twist Mg GB as a function of rotation angle. The GB with a rotation angle of 93.5° was the most energetically stable in the condition from 90° to 100°. Subsequent MD simulations were therefore performed on GBs with the rotation angle set at 93.5°.

Figure 5 shows the results of MD shear tests on the non-segregated GB model. Two Shockley partials moved towards GB2 (Fig. 5(a)) in a 20 ps simulation at an applied stress of

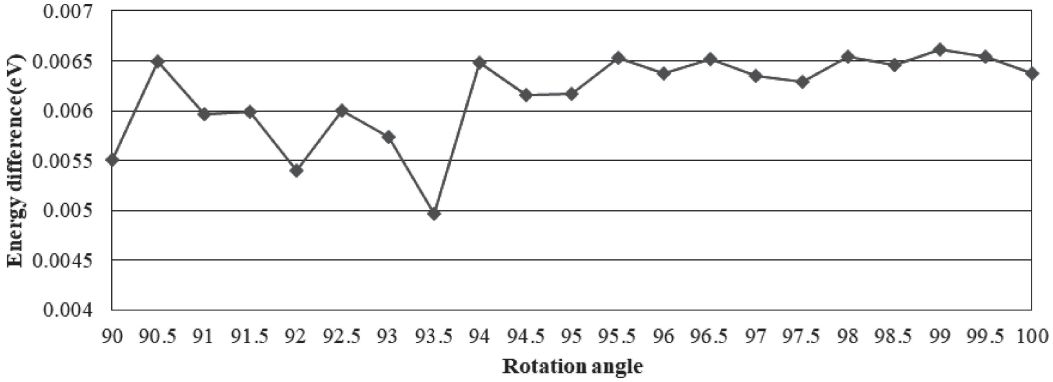

Fig. 4 Variation in energy difference with rotation angle from 90° to 100° in a twist Mg grain boundary.

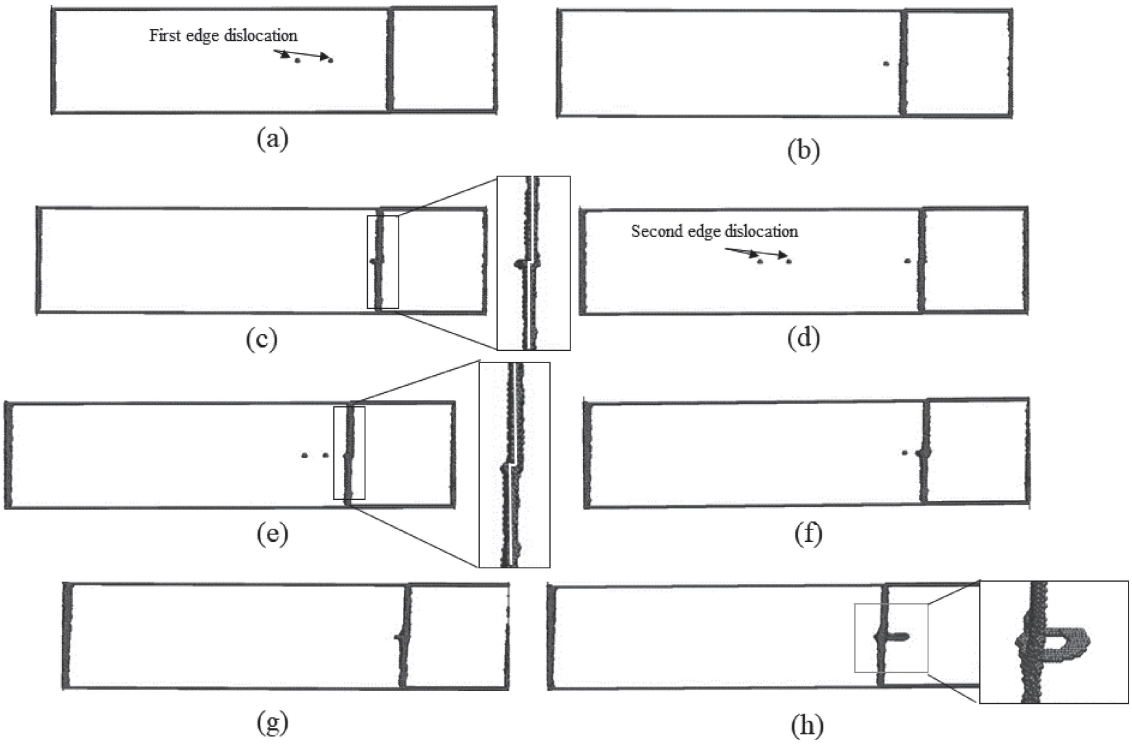

Fig. 5 Interactions between first (a) and (b) and second (c)–(h) edge dislocations and a non-segregated grain boundary during molecular dynamics simulations: (a) 20 ps simulation at 50 MPa, (b) 100 ps simulation at 50 MPa, (c) 20 ps simulation at 100 MPa, (d) 100 ps simulation at 50 MPa, (e) 100 ps simulation at 200 MPa, (f) 15 ps simulation at 300 MPa, (g) 90 ps simulation at 450 MPa and (h) 16 ps simulation at 500 MPa. The atoms are coloured according to the CNA analysis, with the atoms comprising the fcc, hcp, and bcc structures not shown.

50 MPa. The leading partial dislocation was absorbed into the GB2 in a 100 ps simulation at 50 MPa (Fig. 5(b)). After adsorption of the leading partial, the trailing partial was adsorbed in a 20 ps simulation at 100 MPa (Fig. 5(c)). A step was generated at the GB2, as shown in Fig. 5(c), which corresponds with previous results in fcc metals.[11] The emission, reflection or transfer of a dislocation occurs under applied stress or stress concentration after the absorption of a dislocation.[23,24] In this study, however, these events did not occur even under a high applied stress of 900 MPa. An additional edge dislocation was generated in the same way as the generation of the first edge dislocation to further investigate the interactions between edge dislocations and twist GBs (Fig. 5(d)). Figure 5(e) shows the result of a 100 ps simulation at 200 MPa, where the second edge dislocation moved to GB2. The leading partial dislocation of the second dislocations was adsorbed in a 15 ps simulation at 300 MPa (Fig. 5(f)), and the trailing partial of the second dislocation was adsorbed in a 90 ps simulation at 450 MPa (Fig. 5(g)). Finally, a dislocation loop was emitted from the GB2 in a 16 ps simulation at 500 MPa (Fig. 5(h)). Thus, two dislocations were absorbed to generate the emission of one dislocation from the GB. In the present simulations, the applied stresses over 50 MPa were much higher than the Peierls stress of Mg. This is because the high stress is needed for overcoming repulsive interactions between the edge dislocation and the GB.[25]

The Al- and Fe-segregated GBs showed almost the same dislocation absorption behaviour as that of the non-segregated GB in that the adsorption of the first and second edge dislocations into the GB was also observed in both Al- and Fe-segregated GBs. However, the dislocation absorption was generated at a lower applied stress in the Al- and Fe-segregated GBs. For example, the second dislocation was absorbed under a lower applied stress of 350 MPa in the high-concentration Al-segregated GB although this dislocation absorption occurred at 450 MPa in the non-segregation GB (see Table 1). Thus, the absorption of dislocations into the GB was enhanced by the segregation of Al and Fe.

Except for the low-concentration Fe-segregated GB, dislocations were not emitted after the absorption of two dislocations in the Al- and Fe-segregated GBs even under high applied stresses of over 700 MPa. For comparison, dislocation emission occurred at 500 MPa for the non-segregated GB (see Table 1). This suggests that dislocation emission from the GB is suppressed by the segregation of Al and Fe.

4. Discussion

In non-segregated Mg GBs, no dislocation was emitted from the GB when one edge dislocation was adsorbed into the GB, and a dislocation loop was emitted after the adsorption of a second dislocation. The adsorption of one dislocation is enough to emit a dislocation from a tilt GB and a twin GB.[3–8] The dislocation loop emitted from the GB became a dislocation line (Fig. 6) and the emitted dislocation was found to be an edge dislocation whose Burgers vector was $1/3\langle 1\bar{2}10\rangle$. Therefore, the emitted dislocation was a prismatic $\langle a\rangle$ dislocation. In this model, grain 2 was rotated

Table 1 The applied stresses for absorption of first dislocation, for absorption of second dislocation and for dislocation emission, the grain boundary energy, and the grain boundary width in non-segregated and Al- and Fe-segregated twist Mg grain boundaries, where the concentrations of segregated elements are 0.1 and 0.2 atom%.

Segregated element	Concentration (atom%)	Applied stress for adsorption of first dislocation (MPa)	Applied stress for adsorption of second dislocation (MPa)	Applied stress for dislocation emission (MPa)	Grain boundary energy (mJ/m^2)	Grain boundary width (nm)
Al	0.2	50	350	Not emitted	-1645	2.70
Fe	0.2	50	400	Not emitted	-704	2.22
Al	0.1	50	400	Not emitted	-550	2.22
Fe	0.1	50	450	450	-806	1.79
No segregation	-	100	450	500	300	0.68

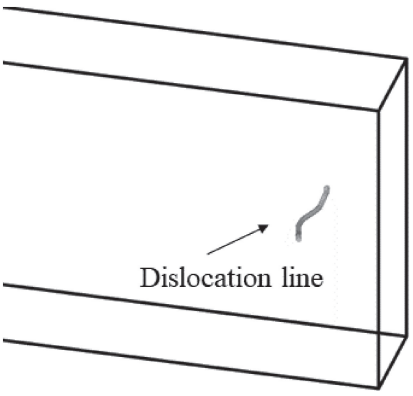

Fig. 6 Dislocation emitted from a non-segregated grain boundary.

about 90° from grain 1 and prismatic plane was almost parallel along applied stress. The GB structure has ordered GB structure after adsorption of the first dislocation (Fig. 5(a)). Therefore, slip transfer of basal slips in matrix into prismatic slip in GB region is easy under applied stress of σ_{zy}. This parallel nature of basal and prismatic planes on the border of GB2 leads to adsorption of basal ⟨a⟩ dislocation into emission of prismatic ⟨a⟩ dislocation.

The critical resolved shear stress for prismatic dislocations is different from that for basal dislocations in hcp metals.[26] First-principle simulations showed that the unstable stacking fault energy (USFE) for prismatic ⟨a⟩ slip is larger than that for basal ⟨a⟩ slip in Mg.[27] In the study, the USFE of prismatic ⟨a⟩ slip is about 2.3 times larger than that for basal ⟨a⟩ slip. Also, a ratio of the maximum gradient along the generalized stacking fault energy (GSFE) for prismatic ⟨a⟩ slip to that for basal ⟨a⟩ slip is about 1.7. Therefore, the emissions of a prismatic ⟨a⟩ dislocation will require a higher stress than the emission of basal ⟨a⟩ dislocation. This suggests that the excessive stress concentration caused by the adsorption of two edge dislocations is necessary for the emission of a prismatic slip dislocation.

Next, we consider the effects of segregated elements on dislocation adsorption and emission. Chandra *et al.*[11] reported that both dislocation adsorption and emission are determined by the GB energy. Table 1 shows that although there seems to be some correlation between the GB energy and the applied stress for dislocation adsorption and emission, much deviation is seen especially in the low-concentration Fe-segregated GB, which indicates that dislocation adsorption and emission cannot be determined by the GB energy alone in segregated GBs. This is because the GB energy of a segregated GB depends not only on mechanical effects, but also on the chemical effects of segregated elements.[1,2] It is difficult to distinguish clearly between the mechanical and chemical effects in MD simulations. Note that the GB width varied with GB segregation (Table 1). The GB width gives an indication of the magnitude of the mechanical effect because it is related to the long-range stress field. The applied stress for dislocation adsorption tended to decrease as the GB width increased, which means that dislocation absorption is enhanced by the mechanical effect. This corresponds with the result in fcc metals.[11]

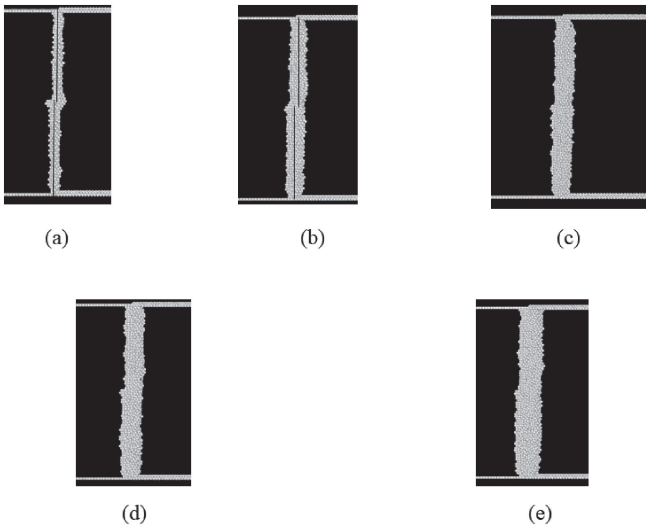

Fig. 7 Grain boundary structure after adsorption of first dislocations: (a) non-segregated GB, (b) low-concentration Fe-segregated GB, (c) low-concentration Al-segregated GB, (d) high-concentration Fe-segregated GB, and (e) high-concentration Al-segregated GB. The atoms are coloured according to the CNA analysis, with the atoms comprising the fcc, hcp and bcc structures not shown.

Figure 7 shows GB2 after the adsorption of the first dislocation. The steps that were caused by the adsorption of the first dislocation were clearly found at the GB, whose width was small, but these steps became unclear in GBs with larger widths. When an edge dislocation was absorbed into the GB, a displacement that is as large as the Burgers vector was generated in the GB. It is more difficult to generate such a displacement in a narrow GB than in a wider one because of the greater disturbance to the GB structure in the narrower GB. This suggests that dislocation adsorption is mainly determined by mechanical effects.

For dislocation emission, the inverse correlation can be seen, that is, the dislocations were not emitted from GBs with large widths. This cannot be explained by the mechanical effect. The potential energy around the GB was examined to determine the chemical effects of segregated elements on dislocation emission (Fig. 8). Dislocations were not emitted from the GBs with low potential energy, which suggests that dislocation emission is suppressed by strong chemical binding between Mg atoms and those of the segregated species. In fact, Mg–Al chemical binding suppresses dislocation emission from the GB by reducing the potential energy.[28] First-principles calculation showed that Al reduces GSFE of Mg via chemical effects.[29] Therefore, chemical effects therefore seem to be the dominant factor in dislocation emission.

For dislocation adsorption, the interactions between a dislocation and a GB are governed by the randomness of GB structure, that is, by mechanical effects. This is because dislocation adsorption needs a large variation in GB structure (Fig. 7). By contrast, the short-range stress fields caused by chemical binding effects are the dominant factors for dislocation emission because atomic shuffling[30–32] or local distortion of the GB structure[33,34] plays a critical role in dislocation emission. Dislocation emission from segregated GBs may thus be qualitatively different from the behaviour in non-segregated GBs because of the dominance of chemical effects in the plastic deformation in segregated GBs.[35]

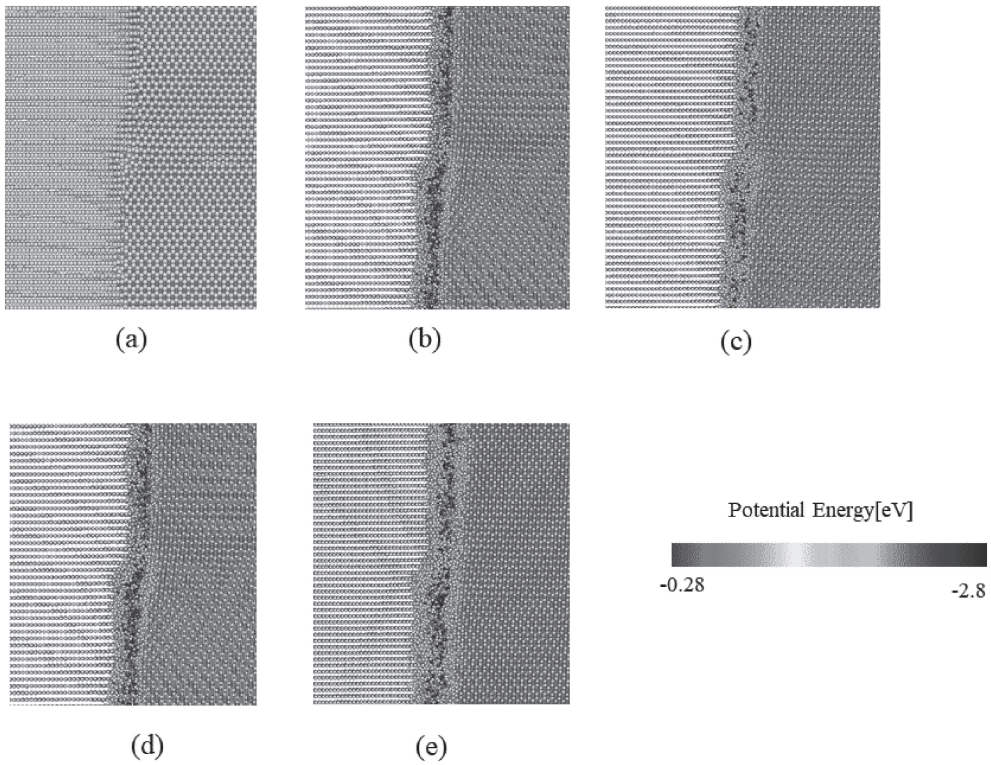

Fig. 8 Potential energies around a grain boundary after adsorption of second dislocations: (a) non-segregated GB, (b) low-concentration Fe-segregated GB, (c) low-concentration Al-segregated GB, (d) high-concentration Fe-segregated GB, and (e) high-concentration Al-segregated GB.

Further research including GB structure analysis for various segregated GBs and first-principles analyses for obtaining electronic point of view is needed to better understand dislocation emission from segregated GBs.

5. Conclusions

MD shear test simulations were performed to investigate the interactions between edge dislocations and twist GBs in Mg. After two basal dislocations were adsorbed into a non-segregated GB, a prismatic dislocation was emitted from the GB. Dislocation adsorption in the GB was enhanced by Al and Fe segregation, while dislocation emission from the GB was suppressed by the segregation. The simulations suggest that dislocation adsorption is mainly determined by mechanical effects, and dislocation emission strongly depends on chemical effects.

Acknowledgments

The work was supported by JSPS KAKENHI Grant Number 19K23570.

REFERENCES

1) A.Y. Lozovoi, A.T. Paxton and M.W. Finnis: Phys. Rev. B **74** (2006) 155416.
2) L. Zhong, R. Wu, A.J. Freeman and G.B. Olson: Phys. Rev. B **62** (2000) 13938.
3) N. Miyazawa, S. Suzuki, M. Mabuchi and Y. Chino: J. Appl. Phys. **122** (2017) 165103.
4) T. Yoshida, M. Yuasa, M. Mabuchi and Y. Chino: J. Appl. Phys. **118** (2015) 034304.
5) Z.-H. Jin, P. Gumbsch, E. Ma, K. Albe, K. Lu, H. Hahn and H. Gleiter: Scr. Mater. **54** (2006) 1163–1168.
6) Z.-H. Jin, P. Gumbsch, K. Albe, E. Ma, K. Lu, H. Gleiter and H. Hahn: Acta Mater. **56** (2008) 1126–1135.
7) M. Chassagne, M. Legros and D. Rodney: Acta Mater. **59** (2011) 1456–1463.
8) M.P. Dewald and W.A. Curtin: Philos. Mag. **87** (2007) 4615–4641.
9) J.F. Nie, Y.M. Zhu, J.Z. Liu and X.Y. Fang: Science **340** (2013) 957–960.
10) S. Chandra, M.K. Samal, V.M. Chavan and R.J. Patel: Mater. Sci. Eng. A **646** (2015) 25–32.
11) S. Chandra, N. Naveen Kumar, M.K. Samal, V.M. Chavan and R.J. Patel: Philos. Mag. **96** (2016) 1809–1831.
12) S. Plimpton: J. Comput. Phys. **117** (1995) 1–19.
13) B. Jelinek, S. Groh, M.F. Horstemeyer, J. Houze, S.G. Kim, G.J. Wagner, A. Moitra and M.I. Baske: Phys. Rev. B **85** (2012) 245102.
14) J. Li: Modelling Simul. Mater. Sci. Eng. **11** (2003) 173.
15) A. Stukowski: Modelling Simul. Mater. Sci. Eng. **18** (2010) 015012.
16) J.D. Honeycutt and H.C. Andersen: J. Phys. Chem. **91** (1987) 4950–4963.
17) Y.N. Osetsky and D.J. Bacon: Modelling Simul. Mater. Sci. Eng. **11** (2003) 427.
18) A. Stukowski and K. Albe: Modelling Simul. Mater. Sci. Eng. **18** (2010) 085001.
19) A. Stukowski, V.V. Bulatov and A. Arsenlis: Modelling Simul. Mater. Sci. Eng. **20** (2012) 085007.
20) A.J. Detor and C.A. Schuh: Acta Mater. **55** (2007) 4221–4232.
21) R. Kirchheim: Acta Mater. **50** (2002) 413–419.
22) H. Faraoun, G. Vincent, C. Esling and H. Aourag: Scr. Mater. **54** (2006) 865–868.
23) M.D. Sangid, T. Ezaz and H. Sehitoglu: Mater. Sci. Eng. A **542** (2012) 21–30.
24) Q. Yin, Z. Wang, R. Mishra and Z. Xia: AIP Adv. **7** (2017) 015040.
25) F. Wang, C.D. Barrett, R.D. McCabe, H.E. Kadiri, L. Capolungo and S.R. Agnew: Acta Mater. **165** (2019) 471–485.
26) M.H. Yoo: Metall. Trans. A **12** (1981) 409–418.
27) H.Y. Wang, N. Zhang, C. Wang and Q.C. Jiang: Scr. Mater. **65** (2011) 723–726.
28) N. Miyazawa, T. Yoshida, M. Yuasa, Y. Chino and M. Mabuchi: J. Mater. Res. **30** (2015) 3629–3641.
29) M. Yuasa, Y. Chino and M. Mabuchi: J. Mater. Res. **29** (2014) 2576–2586.
30) L. Wan and S. Wang: Phys. Rev. B **82** (2010) 214112.
31) H. Van Swygenhoven, P.M. Derlet and A. Hasnaoui: Phys. Rev. B **66** (2002) 024101.
32) P.M. Derlet, H. Van Swygenhoven and A. Hasnaoui: Philos. Mag. **83** (2003) 3569–3575.
33) J.A. Hurtado, B.R. Elliott, H.M. Shodja, D.V. Gorelikov, C.E. Campbell, H.E. Lippard, T.C. Isabell and J. Weertman: Mater. Sci. Eng. A **190** (1995) 1–7.
34) D.E. Spearot, K.I. Jacob and D.L. McDowell: Acta Mater. **53** (2005) 3579–3589.
35) M. Yuasa and M. Mabuchi: Mater. Trans. **52** (2011) 1369–1373.